Talanta 83 (2011) 1501–1506

Contents lists available at ScienceDirect

Talanta

journal homepage: www.elsevier.com/locate/talanta

Electrochemical impedance spectroscopy detection of lysozyme based on electrodeposited gold nanoparticles

Zhengbo Chen, Lidong Li*, Hongtao Zhao, Lin Guo*, Xiaojiao Mu

School of Chemistry and Environment, Beijing University of Aeronautics and Astronautics, Xueyuan Rd. #37, Haidian District, Beijing, 100191, China

ARTICLE INFO

Article history:
Received 28 August 2010
Received in revised form
15 November 2010
Accepted 18 November 2010
Available online 26 November 2010

Keywords:
Aptamer
Electrochemical impedance spectroscopy
Gold nanoparticles
Lysozyme

ABSTRACT

A simple, highly sensitive, and label-free electrochemical impedance spectroscopy (EIS) aptasensor based on an anti-lysozyme-aptamer as a molecular recognition element, was developed for the detection of lysozyme. Improvement in sensitivity was achieved by utilizing gold nanoparticles (AuNPs), which were electrodeposited onto the surface of a gold electrode, as a platform for immobilization of the aptamer. To quantify the amount of lysozyme, changes in the interfacial electron transfer resistance (R_{et}) of the aptasensor were monitored using the redox couple of an $[Fe(CN)_6]^{3-/4-}$ probe. The R_{et} increased with lysozyme concentration. The plot of R_{et} against the logarithm of lysozyme concentration is linear over the range from 0.1 pM to 500 pM with a detection limit of 0.01 pM. The aptasensor also showed good selectivity for lysozyme without being affected by the presence of other proteins.

1. Introduction

Lysozyme is an abundant protein widely distributed in nature. So far, it has been found in mammalian tissues and secretions, and in organisms as diverse as insects, bacteria, viruses and plants [1]. Lysozyme is well known for its muramidase activity which hydrolyzes the bond between N-acetylglucosoamine and N-acetyl muramic acid leading to the degradation of peptidylglycan in the cell wall of Gram-positive bacteria and has thus been termed, the "body's own antibiotic". In the human body, it also has other physiological and pharmaceutical functions, such as anti-inflammatory, anti-viral, immune modulatory, anti-histaminic and anti-tumor activities [2]. In mammals, lysozyme is produced by the cytoplasmic granules of most cells and is present in all body fluids and blood at 0.5–2.0 mg/ml [3]. Change in lysozyme amount can be a former marker of some health problems. It was reported that lysozyme concentration in serum and urine increased in case of leukemia [4] and several kidney problems [5]. In addition, Porstmann et al. reported that lysozyme concentration in cerebrospinal fluid increased in meningitis patients [6]. Serra et al. [7] reported that lysozyme may be a new prognostic factor in patients with breast cancer. Recently, antibodies against to citrullinated variants of lysozyme were found in rheumatoid arthritis patients [8]. Therefore, detection of lysozyme has been getting importance and developing new, rapid, cheap and effective biosensors have been under investigation.

As a new class of single-stranded DNA/RNA molecules, aptamers are short nucleic acid ligands artificially selected for their high specificity and affinity for a wide range of target molecules including proteins, drugs, small molecules, inorganic ions and even cells. They are excellent alternatives to other recognition molecules, such as antibodies, for numerous reasons, for example, the ease of aptamer production, storage, and modification; their small size and chemical simplicity; their target versatility; and their relative resistance to denaturation and degradation. With these advantages, numerous aptamers have been created as ideal recognition probes to detect a broad range of analytes [9,10].

Electrochemical impedance spectroscopy (EIS) has become an increasingly popular electrochemical technique for the investigation of bulk and interfacial electrical properties of any kind of solid or liquid material which is connected to, or part of, an appropriate electrochemical transducer [11]. EIS can be used to monitor the different stages, including the different biosensor fabrication steps, and the detection of a recognition event when an immobilized molecule interacts with analytes. EIS can also be utilized analytically, to measure changes in the electrical properties of the biosensor under various analyte concentrations [12,13]. Compared to other electrochemical methods including cyclic voltammetry (CV), differential pulse voltammetry (DPV) and square-wave voltammograms (SWV), EIS possesses unique advantages, such as ease of signal quantification, an ability to separate the surface binding events from the solution impedance, and less destruction to the biological interactions being measured, and most importantly,

* Corresponding authors. Tel.: +86 10 82338162; fax: +86 10 82338162.
E-mail addresses: lilidong@buaa.edu.cn, xhlili@163.com (L. Li), guolin@buaa.edu.cn (L. Guo).

0039-9140/$ – see front matter © 2010 Elsevier B.V. All rights reserved.
doi:10.1016/j.talanta.2010.11.042

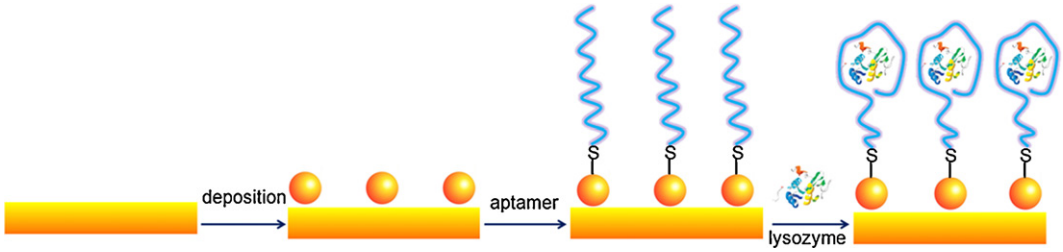

Fig. 1. Schematic representation of an aptasensor with fabrication steps and performance.

redox marker-free on the DNA strand [14]. An EIS biosensor for the determination of lysozyme with a detection limit of 0.07 nM has previously been reported [13].

One promising approach to improving the sensitivity of aptasensors is to utilize nanomaterials for immobilization of the DNA probes [15]. Compared to other types of nanoparticles, AuNPs are superior for many reasons such as electrical conductivity, biocompatibility and ease of self-assembly through a thiol group. AuNPs can also increase the active surface area of the electrode and the amount of immobilized DNA probes [16]. Aptasensors based on a modification of gold nanoparticles for the detection of analytes have been reported by several groups [17–19]. In these cases, the AuNPs were prepared by a chemical method and then modified on the surface of the electrodes through physical adsorption or chemical linking. However, owing to the need for AuNP preparation prior to immobilization, the process of immobilization is time-consuming, and usually requires at least 10 h [14,17,19–21]. Direct electrochemical deposition of AuNPs onto the electrode surface is a very useful way to create a nanomaterial platform in situ for the fabrication of aptasensors [22,23].

Herein, we report a fabrication method for an impedimetric aptasensor based on an anti-lysozyme aptamer and the electrochemical deposition of AuNPs onto the electrode surface. The immobilization of the recognition element introduces electrical insulation and kinetic-transfer barriers at the electrode surface. The transduction principle is based on electron-transfer resistances in the presence of an $[Fe(CN)_6]^{4-/3-}$ redox couple, which can be measured by electrochemical impedance spectroscopy. When we compared aptamer/AuNP/gold electrode with aptamer/gold electrode for the detection of lysozyme, we found that the former presented a lower detection limit and higher sensitivity.

2. Experimental

2.1. Reagents and apparatus

The single strand DNA oligonucleotide (sequence designed by Ellington and co-workers [24]) was synthesized by TaKaRa Biotechnology (Dalian, China) Co., Ltd. The sequence of oligonucleotide employed was: 5′-(SH)-$(CH_2)_6$–ATC TAC GAA TTC ATC AGG GCT AAA GAG TGC AGA GTT ACT TAG-3′. Lysozyme in egg white was supplied by CNS Bioservices Co., Ltd. Tris-(2-carboxyethyl) phosphine hydrochloride (TCEP) was obtained from Alfa Aesar. Bovine serum albumin (BSA), bovine serum hemoglobin (BHb), thrombin, and lysozyme were purchased from CNS Bioservices Co., Ltd.

A CHI 660C electrochemical workstation (Chenhua Instruments Co., Shanghai, China) was used for the electrochemical measurements. All experiments were performed using a conventional three-electrode system with a fabricated aptasensor or bare gold (diameter, 2 mm) as the working electrode, Ag/AgCl (sat. KCl) as the reference electrode, and a platinum counter electrode. All potentials were referred to the reference electrode.

2.2. Fabrication of the aptasensor

Prior to electrodeposition of gold nanoparticles, the gold electrode was cleaned in the piranha solution (v/v, 3:1 H_2SO_4/H_2O_2, see safety considerations) at 90 °C for 5 min [25], followed by rinsing thoroughly with a copious amount of deionized water, and drying under flowing nitrogen gas. Next, the electrode was polished with 1, 0.3, 0.05 μm alumina powders, respectively, followed by sonication in ethanol and deionized water, and electrochemical cleaning (a series of oxidation and reduction cycles in 0.5 M H_2SO_4 with the potential between −0.2 and +1.5 V at 0.1 V/s). Then, the pretreated electrode was immersed into the $HAuCl_4$ (6 mM) solution containing 0.1 M KNO_3, where the electrodeposition was performed under a cyclic voltammetric mode at room temperature. A range of potentials from −0.2 to −1.2 V was applied for 20 cycles at 50 mV/s. An nitrogen atmosphere was kept over the solution during preparation of AuNPs. For immobilization of aptamer, the electrode was incubated in 20-μL aptamer in immobilization buffer solution (I-B: 20 mM Tris–HCl, pH 7.41 with 140 mM NaCl, 20 mM MgCl and 20 mM KCl) for 14 h at 100% humidity, and then washed with deionized water, followed by drying under an N_2 stream. Prior to the use of the anti-lysozyme aptamer, the aptamer (1 μM) including 1 mM TCEP in I-B which was used to reduce disulfide bond oligos was heated to 90 °C for 6 min and then gradually cooled to room temperature. This heating and cooling step is essential to maintain the structural flexibility of the aptamer for binding lysozyme [12]. Non-binding aptamers were removed by rinsing with I-B and deionized water. The resulting electrode was employed as an aptasensor. For lysozyme assays, the aptamer/AuNP/gold electrode was incubated in a 10-μL droplet of various concentrations of lysozyme in I-B and kept for 30 min at 37 °C. Non-binding lysozyme was removed by rinsing with I-B and deionized water. A schematic representation of aptasensor with fabrication steps and performance is displayed in Fig. 1.

2.3. Electrochemical measurements

All electrochemical measurements were performed in an electrochemical cell containing 10 ml of 0.2 M PBS, 10 mM $K_4[Fe(CN)_6]$, 10 mM $K_3[Fe(CN)_6]$ (pH 7.00). Electrochemical impedance measurements were taken: the amplitude of the applied sine potential in each case was 5.0 mV, whereas the bias potential of +0.24 V was limited to the formal potential of the redox couple $[Fe(CN)_6]^{3-/4-}$. The Faradic impedance spectroscopy recorded within the frequency from 100 kHz to 0.1 Hz with a sampling rate of 12 points per decade. The concentration of lysozyme was quantified by semicircle diameter. All measurements were carried out at room temperature.

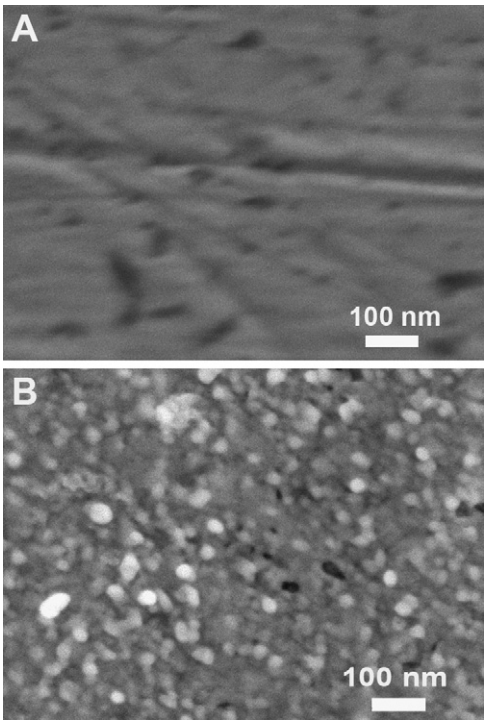

Fig. 2. SEM images of (A) bare gold electrode and (B) AuNP/gold electrode.

3. Results and discussion

3.1. Characterization of aptasensor

The electrochemical deposition of AuNPs on the surface of the gold electrode is described in Section 2.3. A bare gold electrode and an AuNP-modified gold electrode with the same geometric surface areas were characterized by SEM, as shown in Fig. 2(A) and (B), respectively. Comparing with Fig. 2(A), it can be clearly seen that the AuNPs have been electrochemically deposited on the surface of the gold electrode. There average size was 20 nM, with a relative standard deviation of 14%. The microscopic areas of both an AuNP/gold electrode and a bare gold electrode were measured by cyclic voltammogram (CV) in N_2-saturated 0.5 M H_2SO_4, as shown in Fig. 3, assuming that a specific charge of 386 μC/cm^2 was required for gold oxide reduction [26,27]. The total active surface (0.1368 cm^2) of the AuNP/gold electrode was about 2.5-fold higher than that (0.0547 cm^2) of the bare gold electrode.

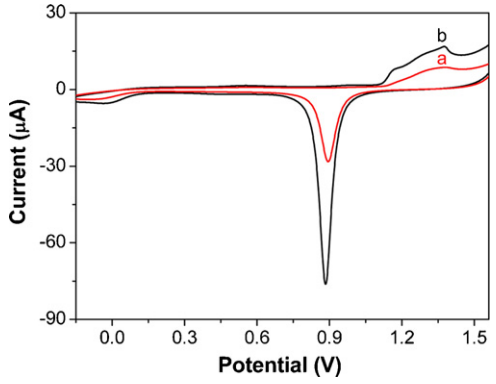

Fig. 3. CVs of (A) bare gold electrode and (B) AuNP/gold electrode in 0.5 M H_2SO_4, scan rate was 50 mV/s.

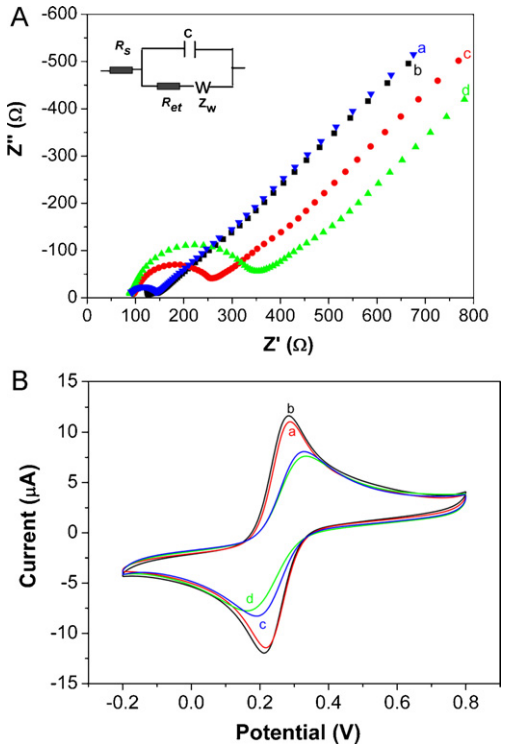

Fig. 4. (A) Nyquist plots of impedance spectra at (a) a bare gold electrode, (b) AuNP/gold electrode, (c) aptamer/AuNP/gold electrode, (d) 0.1 pM lysozyme/aptamer/AuNP/gold electrode. (B) CVs of (a) a bare gold electrode, (b) AuNP/gold electrode, (c) aptamer/AuNP/gold electrode, (d) 0.1 pM lysozyme/aptamer/AuNP/gold electrode in 0.2 M PBS containing 10 mM $K_3Fe(CN)_6$–10 mM $K_4Fe(CN)_6$ (pH 7.0).

In order to monitor each immobilization step and binding step, the corresponding EIS and CV performed in 0.20 M phosphate buffer containing 10 mM $K_3Fe(CN)_6$-10 mM $K_4Fe(CN)_6$ (pH 7.0) were recorded. Fig. 4(A) shows the Nyquist plots of impedance spectra at the same electrode. The bare gold electrode exhibits a very small semicircle at high frequency (curve a). When AuNPs were electrodeposited on the surface of the gold electrode, the electrochemical response is close to a straight line (curve b). After the anti-lysozyme aptamers were self-assembled onto the AuNPs, the R_{et} value significantly increased to 143.1 Ω (curve c). This is probably attributable to the fact that the self-assembled aptamer has a single strand of nucleic acid with negative charges on its phosphate backbone which makes an electrostatic repulsive force to $[Fe(CN)_6]^{3-/4-}$. After 0.1 pM lysozyme was captured onto the surface of the aptasensor, the R_{et} value markedly increased to 232.4 Ω(curve d). An effective barrier to the electron transfer of $[Fe(CN)_6]^{3-/4-}$ in solution provided by the associated bulky lysozyme molecules could account for the increase in R_{et} value of the lysozyme/aptamer/AuNP/gold electrode. Fig. 4(B) shows characterization CVs for each fabrication step of the proposed sensor. As shown in Fig. 4(B) curve a, the $Fe(CN)_6^{3-}$ redox couple showed reversible behavior at a bare gold electrode with a peak-to-peak separation ΔE_p of 68 mV. After AuNPs were electrodeposited on the surface gold electrode (Fig. 4(B), curve b), the reversibility kept the same as the bare gold electrode, and the peak current (I_c = 11.61 μA) even surpassed that of the bare gold electrode (I_c = 11.27 μA) (Fig. 4(B), curve a), suggesting that electro-deposited AuNPs provided the necessary conduction pathways to accelerate the electron transfer between the redox marker and electrode surface. After the anti-lysozyme aptamer was immobilized onto the surface of the AuNP/gold electrode, the electrode exhibited a significant increase in the ΔE_p with a value of 139 mV (Fig. 4(B) curve c),

probably due to the created kinetics barrier between $[Fe(CN)_6]^{3-/4-}$ and the negatively charged phosphate backbones of DNA. Similarly, when 0.1 pM of lysozyme was further adsorbed onto the surface of aptamer/AuNP/gold electrode, ΔE_p value increased to 172 mV. The above results obtained from CVs are in a good agreement with the results obtained from EIS (Fig. 4(A)). In the presence of lysozyme, we found that the change of the R_{et} value in EIS was much more sensitive than that of peak currents in CVs (Fig. S1). Therefore, EIS was utilized in our experiments to improve sensitivity. The impedance data were fitted to a Randle modified equivalent circuit [28], as shown in Fig. 4 (inset), that includes the electrolyte resistance between working and reference electrodes (R_s), Warburg impedance (Z_w), resulting from the diffusion of ions to the interface from the bulk of the electrolyte, electron-transfer resistance (R_{et}), and electrode/electrolyte interface capacitance (C). As indicated from Table S1, the data validation, carried out by the Kramers–Kronig test, proves that experimental results fit reasonably and are in a good agreement with the proposed circuit model ($x^2 \leq 10^{-5}$, Fig. 4 (inset)). While the Z_w gives information about the diffusion of $[Fe(CN)_6]^{3-/4-}$ through the surface layer, the R_s values depend on the solution and the distance between working electrode and reference electrode. C models the capacitive behavior of the double layer replacing the infrequently ideal capacitance and diffusion behavior. However, the deviations from an ideal capacitance ($n = 1$) are reasonably small. The values of R_{et} increase significantly upon increasing lysozyme concentration, reflecting the more hindered charge transfer/marker diffusion. Very small changes are observed for the C and W values.

3.2. Packing density of aptamers

To measure the packing density of DNA probes, a set of different concentrations of $[Ru(NH_3)_6]^{3+}$ were applied onto the surface of the DNA modified electrode. When the DNA-modified surface was exposed to a solution containing $[Ru(NH_3)_6]^{3+}$, the redox cations bound electrostatically to the negatively charged phosphate backbone by replacing the native charge compensation ions (Na^+), and reached an ion-exchange equilibrium. Thus, the packing density of anti-lysozyme aptamer probe can be calculated by the measured charge acquired from the reduction of the $[Ru(NH_3)_6]^{3+}$ that is electrostatically associated with the negatively charged backbone of the aptamer. Fig. S2(A) and (B) shows the cyclic voltammograms of aptamer/AuNP/gold electrodes incubated in varying concentrations of $[Ru(NH_3)]_6^{3+}$ from 2 μM to 10 μM and the cyclic voltammograms of aptamer/gold electrode incubated in varying concentrations of $[Ru(NH_3)]_6^{3+}$ from 2 μM to 6 μM, respectively. As shown in Fig. S2, the peak current increases with increasing concentration, and at 10 μM of $[Ru(NH_3)]_6^{3+}$ for aptamer/AuNP/gold electrode (or at 6 μM for aptamer/gold electrode), the redox current reaches its maximum value which ensures saturation of the DNA-modified surface with the redox-active complex. Under the saturation conditions, the surface concentration of $[Ru(NH_3)_6]^{3+}$, Γ_{Ru}, can be calculated by the following equations.

$$\Gamma_{Ru} = \frac{Q}{nFA} \quad (1)$$

$$\Gamma_{DNA} = \Gamma_{Ru}(z/m)N_A \quad (2)$$

where Q is the charge which involves redox ions from $[Ru(NH_3)_6]^{3+}$ to $[Ru(NH_3)_6]^{2+}$ obtained by integrating the reduction peak area of surface-bound $[Ru(NH_3)_6]^{3+}$, n is the number of electrons involved in the redox reaction, F is Faraday's constant, A is the microscopic area of the electrode, z is the valence of the redox marker $[Ru(NH_3)_6]^{3+}$, m is the number of bases in the DNA probes, and N_A is the Avogadro's constant. By above equations, the packing densities of aptamers immobilized on AuNPs-modified electrode and bare electrode are 3.81×10^{12} molecules cm^{-2} and 2.16×10^{12} molecules cm^{-2}, respectively.

3.3. Performance of the aptasensor

To quantitatively assess the detection limit and response range of the lysozyme aptasensor, Fig. 5(A) shows the Nyquist plots of aptamer/AuNP/gold electrode for lysozyme with different concentrations. Fig. 5(B) displays the dependence of R_{et} on the concentration of lysozyme (0.1–500 pM). The inset of Fig. 5(B) shows R_{et} is linear with logarithm of lysozyme concentration over a range from 0.1 pM to 500 pM. The regression equation was $R_{et} = 539.676 + 269.426 \log C$ (unit of C, pM) and the regression coefficient (r) was 0.991. The detection limit for lysozyme was 0.01 pM as calculated in terms of the 3σ rule [29]. In order to demonstrate that the sensitivity of aptasensor was improved by the application of AuNPs, EIS was also performed on the aptamer/Au electrode. As shown in Fig. 5(C) and (D), the R_{et} is linear with logarithm of lysozyme concentration over the range from 5 nm to 500 nM for aptamer/Au electrode. The regression equation was $R_{et} = 882.986 + 228.224 \log C$, and the regression coefficient was 0.985. The detection limit for lysozyme was 0.003 nM, which is still much lower than the previously reported value (0.07 nM) [11]. Note that the sensitivity of lysozyme detection for the aptasensor which used AuNPs electrodeposited on a gold electrode was higher than the sensitivity obtained for the aptasensor on the bare gold electrode. This can be attributed to the fact that the packing density of aptamer immobilized on the surface of AuNPs (3.81×10^{12} molecules cm^{-2}) was higher than that on the bare gold electrode (2.16×10^{12} molecules cm^{-2}).

3.4. Selectivity of the apatasensor

Not only does the aptasensor have to be sensitive to different concentrations of the analyte, also it must be specific. Experiments were thus conducted on BSA, BHb, and thrombin, to serve as interference compound that belong to the protein family with lysozyme. These proteins all exist in the same environment such as blood, and have properties similar to those of lysozyme. Lysozyme strongly associates with proteins with low isoelectric points (isoelectric points of lysozyme, thrombin, BSA, and BHb are about 11, 7, 7.8 and 7.1, respectively). Thus, they serve as excellent control to assess the specificity of the aptamer/AuNP/gold electrode for the detection of lysozyme. The responses of the aptamer/AuNP/gold electrode to 1 pM lysozyme and the mixture of 1 pM lysozyme–1 pM thrombin–1 pM BSA–1 pM BHb were checked, respectively. The results showed that the R_{et} value in a mixture of 1 pM lysozyme–1 pM thrombin–1 pM BSA–1 pM BHb was very close to that obtained in 1 pM lysozyme, as shown in Fig. 6. This indicates that the aptasensor has a high selectivity.

3.5. Stability of the aptasensor

Stability studies of the proposed aptasensor have been carried out by our group. The results indicate that, in the presence of lysozyme, the response of the aptasensor to 0.1 pM lysozyme was 84% of the original signal after it had been stored in I-B at 4 °C for one month (Fig. 7).

3.6. Application of the aptasensor

To investigate the feasibility of this biosensor for the analysis of biological samples, the content of lysozyme in egg was examined. Lysozyme is made up of 3.5% content in egg. The lysozyme in an egg white sample was diluted to 0.5 nM and then analyzed by EIS. The R_{et} of detection sample according to the standard curve is 1210 Ω

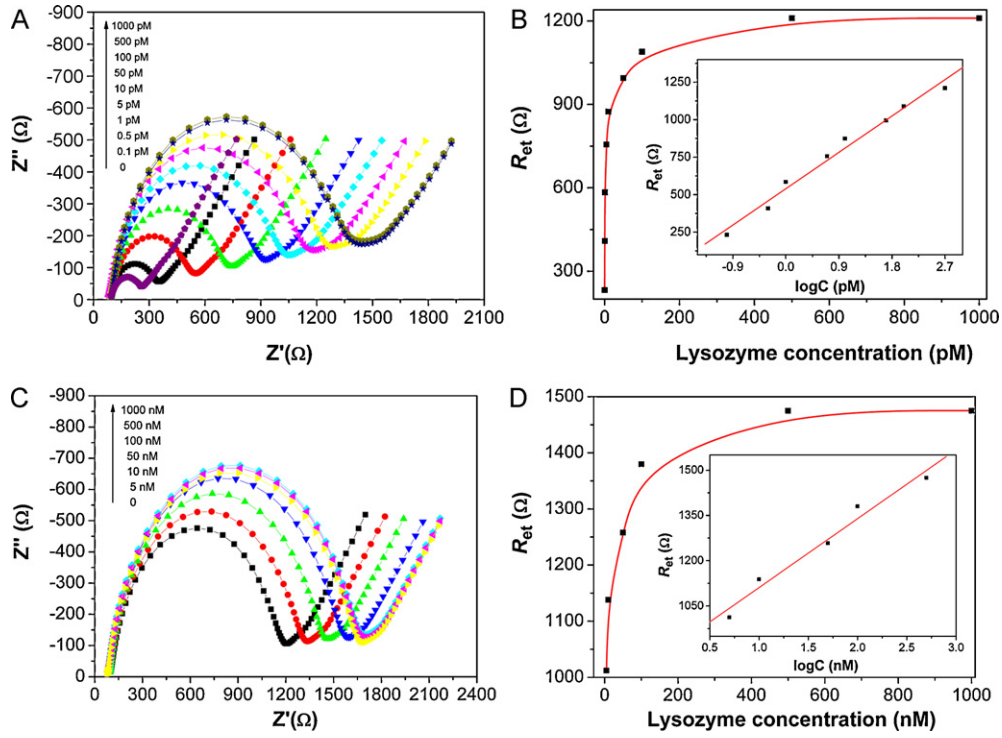

Fig. 5. (A) Nyquist plots of the aptamer/AuNP/gold electrode after interaction with different concentrations of lysozyme from 0.1 pM to 500 pM. (B) The dependence of R_{et} of the aptamer/AuNP/gold electrode on the concentration of lysozyme. The inset shows the R_{et} is linear with logarithm of lysozyme concentration over the range from 0.1 pM to 500 pM. (C) Nyquist plots of the aptamer/gold electrode after interaction with different concentrations of lysozyme from 5 nM to 500 nM. (D) The dependence of R_{et} of the aptamer/gold electrode on the concentration of lysozyme. The inset shows the R_{et} is linear with logarithm of lysozyme concentration over the range from 5 nM to 500 nM.

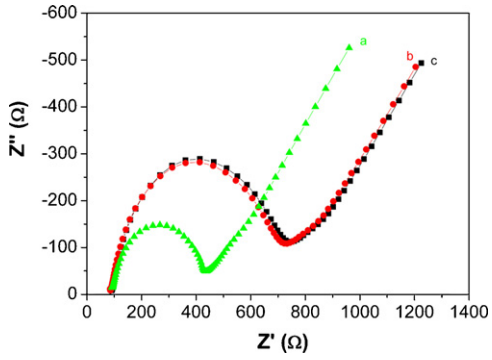

Fig. 6. Nyquist plots of impedance spectra for the aptamer/AuNP/gold electrode after reaction with (A) 0 pM lysozyme, (B) 1 pM lysozyme and (C) a mixture of 1 pM lysozyme–1 pM thrombin–1 pM BSA–1 pM BHb.

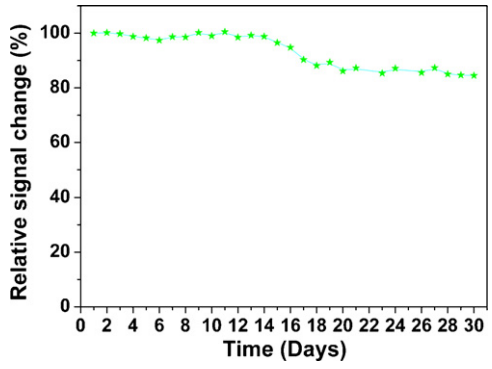

Fig. 7. The time dependence of the relative signal change referring to the original signal of the proposed aptasensor at 0.1 pM lysozyme in the 1st-day measurement.

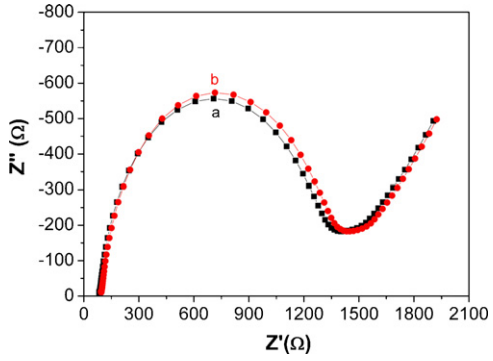

Fig. 8. Nyquist plots of impedance spectra for (A) 0.5 nM lysozyme (in I-B)/aptamer/AuNP/gold electrode, and (B) 0.5 nM lysozyme(in egg white)/aptamer/AuNP/gold electrode.

with a relative error of 2.11% ($n = 3$), as shown in Fig. 8.In view of the activity of lysozyme in egg white, the result is still satisfactory.

4. Conclusions

In conclusion, we developed a simple, sensitive and label-free EIS aptasensor for the detection of lysozyme. This work demonstrated that the sensitivity can be greatly improved by AuNP modification, which can be attributed to the fact that the electrodeposited AuNPs can be used as a platform with 4.4-fold more aptamer immobilization for capturing lysozyme than the platform without AuNP modification. Furthermore, the proposed aptasensor has a very low detection limit of 0.01 pM. Given that EIS aptasensor possesses many advantages such as high sensitivity, selectivity, and stability, this approach could be adapted to aptamer-based detections of other proteins and small molecules.

Acknowledgements

This project was financially supported by National Natural Science Foundation of China (nos. 20903008, 20973019, and 50725208) and the State Key Project of Fundamental Research for Nanoscience and Nanotechnology (2006CB932300).

Appendix A. Supplementary data

Supplementary data associated with this article can be found, in the online version, at doi:10.1016/j.talanta.2010.11.042.

References

[1] M. Schindler, Y. Assaf, N.D. Sharon, M. Chipman, Biochemistry 16 (1977) 423–431.
[2] G.P. Gorbenko, V.M. Loffe, P.K.J. Kinnunen, Biophysics 93 (2007) 140–153.
[3] P. Jolles, EXS 75 (1996) 3–5.
[4] R. Pascual, J. Gee, S. Finch, N. Eng. J. Med. 289 (1973) 1074–11074.
[5] B. Porstmann, K. Jung, H. Schmechta, U. Evers, Clin. Biochem. 22 (1989) 349–355.
[6] G. Horpacsy, J. Zinsmeyer, K. Schroder, M. Mebel, Clin. Chem. 24 (1978) 74–79.
[7] C. Serra, F. Vizoso, L. Alonso, J.C. Rodríguez, L.O. González, M. Fernández, M.L. Lamelas, L.M. Sánchez, J.L. García-Muñiz, A. Baltasar, J. Medrano, Breast Cancer Res. 4 (2002) R16.
[8] J. Ireland, J. Herzog, E.R. Unanue, J. Immunol. 177 (2006) 1421–1425.
[9] J.E. Smith, C.D. Medley, Z.W. Tang, D.H. Shang, C. Lofton, W.H. Tan, Anal. Chem. 79 (2007) 3075–3082.
[10] K. Stadtherr, H. Wolf, P. Lindner, Anal. Chem. 77 (2005) 3437–3443.
[11] E. Katz, I. Willner, Electroanalysis 15 (2003) 913–947.
[12] M.C. Rodriguez, A.N. Kawde, J. Wang, Chem. Commun. (2005) 4267–4269.
[13] Y. Peng, D.D. Zhang, Y. Li, H.L. Qi, Q. Gao, C.X. Zhang, Biosens. Bioelectron. 25 (2009) 94–99.
[14] L.D. Li, Z.B. Chen, H.T. Zhao, X.J. Mu, L. Guo, Sens. Actuators B 149 (2010) 110–115.
[15] H. Wang, C.X. Zhang, Y. Li, H.L. Qi, Anal. Chim. Acta 575 (2006) 205–211.
[16] M.T. Castaneda, S. Alegret, A. Merkoci, Electroanalysis 19 (2007) 743–753.
[17] J.G. Bai, H. Wei, B.L. Li, L.H. Song, L.Y. Fang, Z.Z. Lv, W.H. Zhou, E.K. Wang, Chem. Asian J. 3 (2008) 1935–1941.
[18] Z.Q. Liang, J. Zhang, L.H. Wang, S.P. Song, C.H. Fan, G.X. Li, Int. J. Mol. Sci. 8 (2007) 526–532.
[19] X.X. Li, H.L. Qi, L.H. Shen, Q. Gao, C.X. Zhang, Electroanalysis 20 (2008) 1475–1482.
[20] L.D. Li, H.T. Zhao, Z.B. Chen, X.J. Mu, L. Guo, Anal. Bioanl. Chem. 398 (2010) 563–570.
[21] L. Su, L.Q. Mao, Talanta 70 (2006) 68–74.
[22] C.Z. Li, Y. Liu, J.H.T. Luong, Anal. Chem. 77 (2005) 478–485.
[23] S.F. Liu, Y.F. Li, J.R. Li, L. Jiang, Biosens. Bioelectron. 21 (2005) 789–795.
[24] R. Kirby, E.J. Cho, B. Gehrke, T. Bayer, Y.S. Park, D.P. Neikirk, J.T. McDev-itt, A.D. Ellington, Anal. Chem. 76 (2004) 4066–4075.
[25] A.N. Kawde, M.C. Rodriguez, T.M.H. Lee, J. Wang, Electrochem. Commun. 7 (2005) 537–540.
[26] R. Woods, in: A.J. Bard (Ed.), Electroanalytical Chemistry: A Series of Advances, vol. 9, Marcel Dekker, New York, 1980.
[27] R. Szamocki, A. Velichko, C. Holzapfel, F. Mucklich, S. Ravaine, P. Garrigue, N. Sojic, R. Hempelmann, A. Kuhn, Anal. Chem. 79 (2007) 533–539.
[28] F. Patolsky, M. Zayats, B. Katz, I. Willner, Anal. Chem. 71 (1999) 3171–3180.
[29] H. Kaiser, Pure Appl. Chem. 34 (1973) 35–62.